Article

Cancer Cell

Inhibition of the Mitochondrial Protease ClpP as a Therapeutic Strategy for Human Acute Myeloid Leukemia

Highlights

- ClpP is a mitochondrial protease overexpressed in a subset of AML and stem cells
- Inhibition of ClpP decreases the viability of AML cells with high ClpP expression
- ClpP interacts with mitochondrial respiratory chain proteins and metabolic enzymes
- Genetic knockdown of ClpP impairs oxidative phosphorylation and complex II

Authors

Alicia Cole, Zezhou Wang, ..., Brian Raught, Aaron D. Schimmer

Correspondence

aaron.schimmer@utoronto.ca

In Brief

Cole et al. show that ClpP, a mitochondrial protease, is overexpressed in a large fraction of human acute myeloid leukemias (AMLs) and that inactivation of ClpP selectively kills these AML cells via inhibition of oxidative phosphorylation and mitochondrial metabolism.

Cole et al., 2015, Cancer Cell *27*, 864–876
June 8, 2015
http://dx.doi.org/10.1016/j.ccell.2015.05.004

CellPress

CellPress

Cancer Cell
Article

Inhibition of the Mitochondrial Protease ClpP as a Therapeutic Strategy for Human Acute Myeloid Leukemia

Alicia Cole,[1] Zezhou Wang,[1] Etienne Coyaud,[1] Veronique Voisin,[2] Marcela Gronda,[1] Yulia Jitkova,[1] Rachel Mattson,[1] Rose Hurren,[1] Sonja Babovic,[3] Neil Maclean,[1] Ian Restall,[1] Xiaoming Wang,[1] Danny V. Jeyaraju,[1] Mahadeo A. Sukhai,[1] Swayam Prabha,[1] Shaheena Bashir,[2] Ashwin Ramakrishnan,[1] Elisa Leung,[4] Yi Hua Qia,[5] Nianxian Zhang,[6,12] Kevin R. Combes,[5] Troy Ketela,[7] Fengshu Lin,[1] Walid A. Houry,[4] Ahmed Aman,[8] Rima Al-awar,[8,9] Wei Zheng,[10] Erno Wienholds,[1,11] Chang Jiang Xu,[2] John Dick,[1,11] Jean C.Y. Wang,[1,11] Jason Moffat,[7] Mark D. Minden,[1,11] Connie J. Eaves,[3] Gary D. Bader,[2] Zhenyue Hao,[1] Steven M. Kornblau,[5] Brian Raught,[1] and Aaron D. Schimmer[1,11,*]

[1]Princess Margaret Cancer Centre, Toronto, ON M5G 2M9, Canada
[2]Department of Molecular Genetics, University of Toronto, Toronto, ON M5S 1A8, Canada
[3]Terry Fox Laboratory, British Columbia Cancer Agency and University of British Columbia, Vancouver, BC V5Z 1L3, Canada
[4]Department of Biochemistry, University of Toronto, Toronto, ON M5S 1A8, Canada
[5]Department of Leukemia, The University of Texas MD Anderson Cancer Center, Houston, TX 77030, USA
[6]Department of Bioinformatics and Computational Biology, The University of Texas MD Anderson Cancer Center, Houston, TX 77030, USA
[7]Department of Molecular Genetics, Donnelly Centre for Cellular and Biomolecular Research, Toronto, ON M5S 3E1, Canada
[8]Drug Discovery Program, Ontario Institute for Cancer Research, Toronto, ON M5G 0A3, Canada
[9]Department of Pharmacology and Toxicology, University of Toronto, Toronto, ON M5S 1A8, Canada
[10]National Center for Advancing Translational Sciences, National Institutes of Health, Bethesda, MD 20892, USA
[11]Department of Medicine, University of Toronto, Toronto, ON M5G 2C4, Canada
[12]Present address: Department of Biomedical Informatics, The Ohio State University Wexner Medical Center, Columbus, OH 43210, USA
*Correspondence: aaron.schimmer@utoronto.ca
http://dx.doi.org/10.1016/j.ccell.2015.05.004

SUMMARY

From an shRNA screen, we identified ClpP as a member of the mitochondrial proteome whose knockdown reduced the viability of K562 leukemic cells. Expression of this mitochondrial protease that has structural similarity to the cytoplasmic proteosome is increased in leukemic cells from approximately half of all patients with AML. Genetic or chemical inhibition of ClpP killed cells from both human AML cell lines and primary samples in which the cells showed elevated ClpP expression but did not affect their normal counterparts. Importantly, *Clpp* knockout mice were viable with normal hematopoiesis. Mechanistically, we found that ClpP interacts with mitochondrial respiratory chain proteins and metabolic enzymes, and knockdown of ClpP in leukemic cells inhibited oxidative phosphorylation and mitochondrial metabolism.

INTRODUCTION

The cytoplasmic/nuclear proteasome complex is a well recognized therapeutic target, and proteasome inhibitors have been approved for the treatment of hematologic malignancies (Fisher et al., 2006; O'Connor et al., 2009; Richardson et al., 2005; Vij et al., 2012). Mitochondria also possess a serine protease complex, ClpP, that is structurally similar to the cytoplasmic/nuclear proteasome (Goard and Schimmer, 2014), but little is known about the expression of this complex or the effects of its inhibition in malignant cells.

ClpP is encoded by a nuclear gene, translated in the cytoplasm, and imported into the mitochondrial matrix. There it is assembled into a tetradecamer consisting of seven repeated symmetric rings arranged in a stable double-ringed structure (Corydon et al., 1998; de Sagarra et al., 1999), each end of which

Significance

Perturbations in the cytoplasmic and nuclear proteasome are known to contribute to the acquisition of malignant properties, but the importance of ClpP, a mitochondrial protease with structural homology to the proteasome, has not been established. We have now shown that loss of ClpP does not impact normal hematopoiesis, whereas ClpP inhibition kills human leukemic cells, including those with stem and progenitor activity, which may be attributable to their higher mitochondrial stress and a greater reliance on oxidative phosphorylation. These results suggest that targeting mitochondrial ClpP may be an attractive therapeutic strategy for a subset of human acute leukemias.

is capped by an AAA+ ATPase chaperone, ClpX (Kang et al., 2005). Based on studies of its homologs in bacteria and its structural similarities to the cytoplasmic proteasome, the ClpP complex is thought to degrade damaged or misfolded proteins inside mitochondria.

Inhibition of ClpP in normal mice (Gispert et al., 2013), humans (Jenkinson et al., 2013), and *C. elegans* (Haynes et al., 2007, 2010) has not been found to elicit much loss of viability. For example, *Clpp*$^{-/-}$ mice are viable but display infertility, slight growth retardation, and acquired hearing loss (Gispert et al., 2013). Homozygous *CLPP* mutations have also been described in individuals from three human families (Jenkinson et al., 2013). Similar to the mouse phenotype, these individuals have congenital hearing loss and premature ovarian failure. In contrast, deregulating ClpP activity in certain bacteria, either through inhibition (Zeiler et al., 2012) or increased activation (Conlon et al., 2013), is cytotoxic even when they are dormant or have acquired antibiotic resistance (Conlon et al., 2013).

Recently, we (Skrtić et al., 2011) and others (Lagadinou et al., 2013) demonstrated that leukemic cells, including those with stem and progenitor activity from patients with acute myeloid leukemia (AML) have an increased mitochondrial mass and reliance on oxidative phosphorylation. We therefore initiated a study to identify members of the mitochondrial proteome whose inhibition might reduce the viability of AML cells.

RESULTS

A Genetic Screen Identifies ClpP as Essential for the Viability of Leukemia Cells

We first sought to determine whether short hairpin RNA (shRNA)-mediated knockdown of any of the 1,300 members of the mitochondrial proteome would identify candidates that could reduce the viability of human leukemic cells using K562 cells as targets. Accordingly, we transduced K562 cells with a library of 54,021 shRNAs in barcoded lentiviral vectors targeting 11,255 nuclearly encoded genes. Twenty-one days after transduction, cells were harvested, genomic DNA was isolated, and the relative abundance of shRNA sequences present in the surviving cells was determined by array analysis of the barcodes. shRNAs able to reduce the viability or growth of K562 cells were inferred to be those not represented in the final cell population (Figure S1A). shRNAs targeting BCR and ABL1 were top hits (Figures S1A–S1C), therefore validating the robustness of the screen because K562 cells are dependent on the BCR-ABL1 fusion oncoprotein for survival (Dan et al., 1998). In this screen, 2,422 shRNAs targeted 496 members of the mitochondrial proteome, and of the top 25 targets, four were mitochondrial proteases (NLN, ClpP, PARL, and PITRM1), with two targeting ClpP ranking in the top 1% of all hits in the screen (Figures 1A–1C). In contrast, the mitochondrial matrix protease Lon did not appear as a hit in our shRNA screen, and repetition of this experiment using shRNAs that produced high levels of target knockdown (both protein and mRNA) confirmed that Lon was not required for the growth and viability of TEX, OCI-AML2, or K562 leukemia cells (Figure S1D and data not shown). Therefore, some, but not all, mitochondrial proteases are necessary for the viability of AML cells.

ClpP Is Overexpressed in a Subset of AML Cells and Patient Samples

To investigate ClpP further as a therapeutic target in human AML, we measured ClpP protein expression in 511 primary AML samples and CD34^{+} cells from 21 healthy individuals using reverse-phase protein array. Compared with normal CD34^{+} hematopoietic progenitor cells, ClpP was overexpressed in 45% of the primary AML samples (Figure 1D). Elevated ClpP was not correlated with CD34 expression based on flow cytometry, remission attainment, overall or event-free survival, or remission duration (Figures S1E–S1G and data not shown). Increased expression of ClpP also showed no association with any morphologic subtype, cytogenetic risk group, or mutational profile (Figures 1E and 1F; Figures S1H–S1M).

Increased expression of ClpP in a subset of AML cell lines and patient samples was confirmed by immunoblotting (Figure 1G; Figure S1N). In addition, we demonstrated that *CLPP* mRNA was increased in a subset of AML cells compared with normal hematopoietic cells and expressed similarly in the bulk and progenitor (CD34^{+}CD38^{-}) populations of primary AML samples (Figure S1O). Gene expression analysis of previously characterized AML patient samples demonstrated that *CLPP* mRNA was similarly expressed in fractions enriched or depleted of leukemic stem cells (LSCs) defined by functional assays ($p = 0.45$) (Figure S1P). Analysis of TCGA data indicated that *CLPP* expression did not correlate with known AML mutations (Table S1).

In primary AML patient samples, higher *CLPP* expression was associated with an increased expression of genes related to the mitochondrial unfolded protein response (mtUPR). This positive correlation was observed in both the LSC^{+} and LSC^{-} fractions of primary AML cells (Figures S1Q and S1R). Therefore, increased ClpP may be a marker of increased mitochondrial stress in a subset of AML patients that is downstream of multiple genetic pathways.

Analysis of the Cancer Cell Line Encyclopedia indicated that *CLPP* was highly expressed in AML cells but also increased in subsets of other hematologic malignancies, including multiple myeloma, various lymphomas, and chronic myeloid leukemia (CML). In addition, *CLPP* was highly expressed in solid tumors such as prostate cancer and sarcomas (Figure S1S). Therefore, ClpP may also be a relevant target for malignancies beyond AML.

Genetic Knockdown of ClpP Reduces the Growth and Viability of AML Cells with High ClpP Expression

We next tested the effects of ClpP knockdown on the growth and viability of AML cells. K562, TEX, OCI-AML2, and HL60 cells were transduced with lentiviral vectors expressing a control sequence or three independent shRNA sequences targeting *CLPP*. The shRNA sequences targeting *CLPP* showed robust target knockdown by both quantitative RT-PCR and immunoblotting (Figures 2A–2D and data not shown). Knockdown of ClpP reduced the growth and viability of the K562, TEX, and OCI-AML2 cells that have high ClpP expression (Figures 2A–2C) but not HL60 cells that express low basal levels of ClpP (Figure 2D). In addition, knockdown of ClpP in TEX cells reduced engraftment into the marrow of non-obese diabetic

A

Gene	# shRNA with >50% depletion	Max depletion (%)
KARS	4	98.41
MAOA	3	93.56
NLN	2	93.25
RAB11B	2	92.93
BCL2	2	92.63
CLPP	2	91.19
VDAC1	2	90.60
ATP5B	1	97.88
HRSP12	1	95.91
SLC25A15	1	95.25
SLC25A29	1	94.86
TRIT1	1	94.42
DHX29	1	93.21
PARL	1	92.99
TXNRD2	1	92.85
CLIC4	1	92.78
ACADSB	1	92.68
TSFM	1	92.45
STAR	1	92.38
OXA1L	1	92.18
TRMU	1	92.10
SPR	1	92.08
COX6B2	1	91.04
PITRM1	1	91.01
ATP5G2	1	90.99

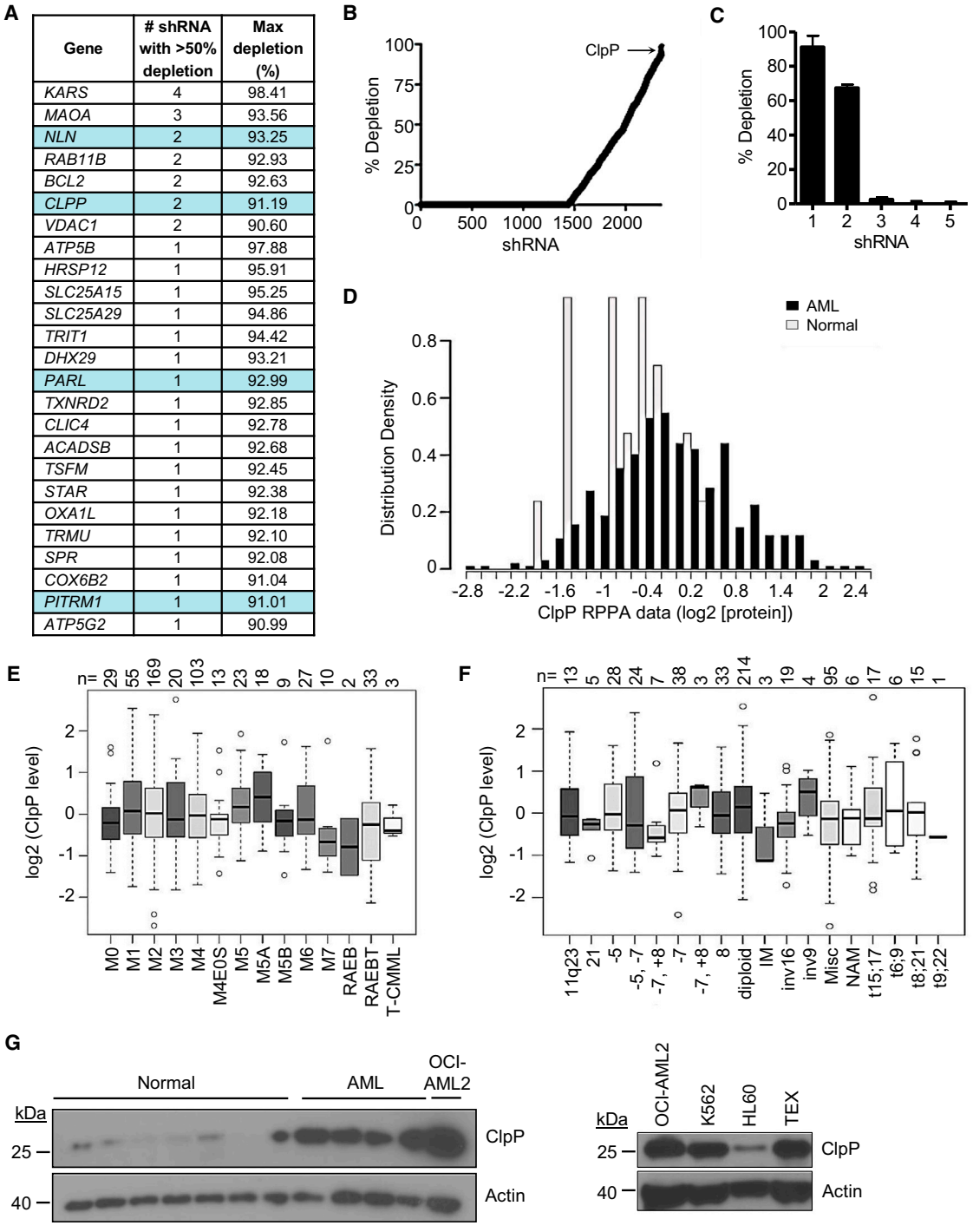

Figure 1. A Genetic Screen Identifies ClpP as Essential for the Viability of Leukemia Cells

(A) The list of top 25 shRNAs targeting the mitochondrial proteome. Max, maximum.

(B) The percent depletion in rank order of the 2,422 shRNAs targeting 496 members of the mitochondrial proteome.

(C) The percent depletion of individual clones in the library targeting ClpP.

(D) Expression of ClpP measured in total cell lysates from 511 primary AML cases and 21 samples of normal $CD34^+$ hematopoietic cells using a reverse-phase protein array.

(E and F) Expression of ClpP in primary AML cases classified based on their morphologic French American British (FAB) subtype (E) or cytogenetic abnormalities (F).

(G) Expression of ClpP protein in total cell lysates prepared from normal hematopoietic cells, primary AML samples, and indicated cell lines by immunoblotting. Error bars represent SD. The box represents the first and third quartiles, whiskers represent the range, the center line represents the median, and the circles represent outliers. See also Figure S1 and Table S1.

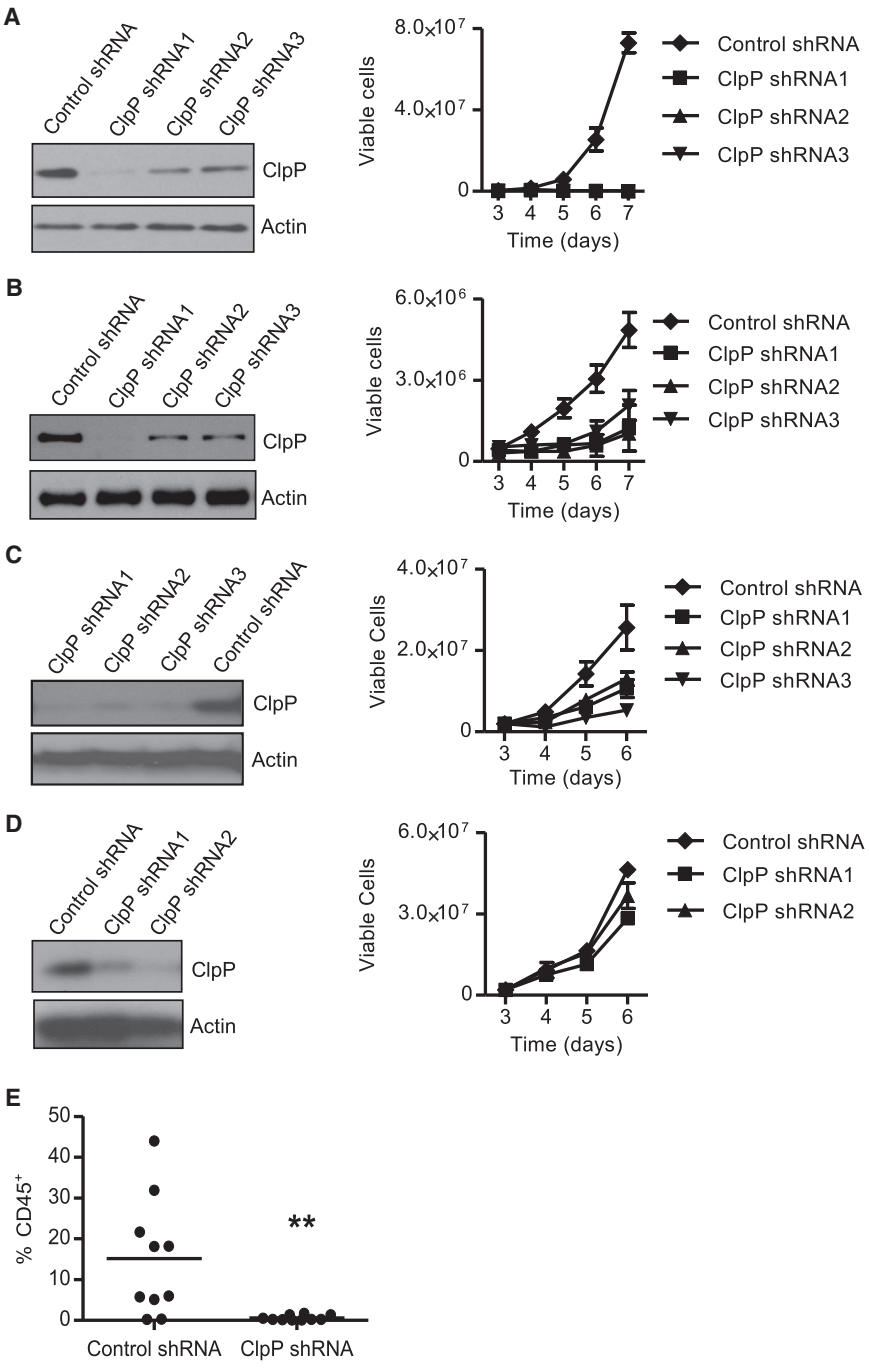

Figure 2. Knockdown of ClpP Reduces the Growth and Viability of AML Cells

(A–D) The expression of ClpP and Actin in TEX (A), OCI-AML2 (B), K562 (C), and HL60 (D) cells 4 days after transduction with lentiviral vectors expressing control shRNA or one of the three shRNAs targeting ClpP were detected by immunoblotting. Viable cell counts of cells seeded 4 days after transduction are shown as mean ± SD. One of three representative experiments is shown.

(E) The percentage of human $CD45^+$ cells in the non-injected femur of sublethally irradiated NOD/SCID-GF mice determined by flow cytometry (n = 10/group). **p = 0.005 by t test. The bar represents mean engraftment.

(NOD)/severe combined immunodeficiency-growth factor (SCID-GF) mice (Figure 2E).

Clpp Knockout Mice Are Viable with Normal Hematopoiesis

To assess the effects of ClpP inhibition on normal hematopoiesis in vivo, we created constitutive ClpP-deficient mice. In wild-type (WT) mice, ClpP protein was expressed at low levels in the bone marrow, lung, kidney, and stomach but was more abundant in the pancreas, colon, testis, brain, and liver (Figure S2A). ClpP was absent in all tested tissues from $Clpp^{-/-}$ mice (Figure S2B). $Clpp^{-/-}$ mice are viable, although slightly smaller than their WT counterparts (Figures S2C and S2D). Therefore, our mice are similar to those obtained by Gispert et al. (2013), who reported that 80% of their $Clpp^{-/-}$ mice survived over 400 days but were infertile and had impaired hearing.

The study by Gispert et al. (2013) did not report the effects of *Clpp* deficiency on hematopoiesis. We therefore studied hematopoiesis in our $Clpp^{-/-}$ mice. $Clpp^{-/-}$ mice had normal numbers of all mature blood cell types in the circulation (Figure 3A) and normal numbers of phenotypically defined ($Lin^-cKit^+Sca1^+$) progenitor cells in the bone marrow (Figure 3B). In vitro colony assays confirmed the presence of equal numbers of progenitors in the bone marrow of WT and $Clpp^{-/-}$ mice (Figure 3C). Likewise, cells from the marrow of $Clpp^{-/-}$ and WT mice had a similar ability to repopulate the marrow of sublethally irradiated congenic W^{41}/W^{41} recipients when assessed in a competitive repopulation assay (Figure 3D). T and B cell function and the number of natural killer (NK) cells were also similar in $Clpp^{-/-}$ and WT mice (Figures S2E–S2G). p16 expression in T cells from $Clpp^{-/-}$ and WT mice was also similar (Figure S2H). This lack of any detectable effect of *Clpp* absence in murine hematopoiesis supports the potential feasibility of using ClpP inhibitors for the treatment of AML.

ClpP Interacts with Respiratory Chain Proteins and Mitochondrial Metabolism Enzymes

The function and substrates of mammalian ClpP are largely unknown. To gain insight into ClpP function, we used the BioID-mass spectrometry (BioID-MS) method to identify ClpP-interacting partners (Roux et al., 2012). To identify interacting proteins using BioID-MS, a protein of interest is fused in-frame with a

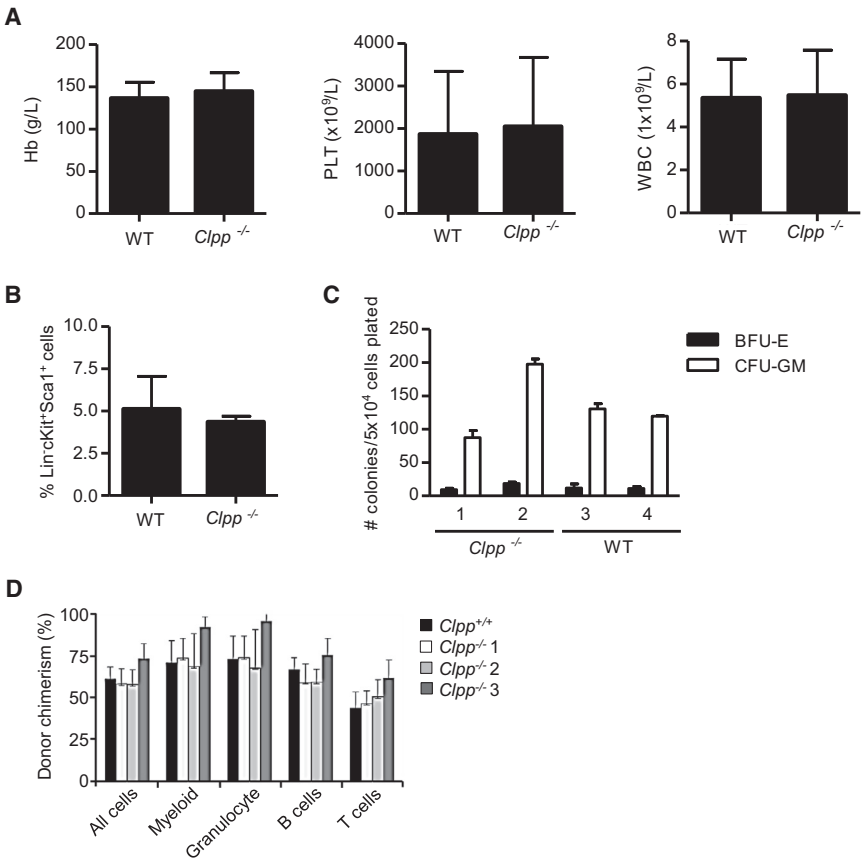

Figure 3. ClpP Knockout Mice Are Viable with Normal Hematopoiesis

(A) Mean ± SD hemoglobin (Hb), platelet (PLT), and WBC counts from peripheral blood samples of WT and *Clpp*$^{-/-}$ mice (n = 4/group).

(B) The frequency of Lin^{-}cKit^{+}Sca1^{+} hematopoietic cells in the bone marrow of WT and *Clpp*$^{-/-}$ mice. Mean ± SD percentages were determined by flow cytometry.

(C) Erythroid and myeloid colony formation from burst-forming unit-erythroid (BFU-E) and colony-forming unit-granulocyte, monocyte (CFU-GM) of hematopoietic cells from WT and *Clpp*$^{-/-}$ mice (n = 3/group) plated in vitro under standard conditions. Mean ± SD colony counts are shown.

(D) The mean ± SD proportions of CD45.2 cells from WT or *Clpp*$^{-/-}$ mice transplanted in sublethally irradiated congenic W^{41}/W^{41} CD45.1 mice measured by flow cytometry.

See also Figure S2.

mutant *E. coli* biotin conjugating enzyme, BirA R118G (or BirA*). BirA* efficiently activates biotin but exhibits a reduced affinity for the activated molecule. Biotinoyl-AMP, therefore, simply diffuses away from BirA* and reacts with nearby amine groups, including those present on lysine residues in neighboring polypeptides. Following stringent cell lysis, biotinylated proteins can be affinity-purified and identified using mass spectrometry.

From this protein interaction screen, we identified 191 mitochondrial ClpP-interacting proteins, 49 of which preferentially interacted with WT or mutant ClpP over the unrelated mitochondrial matrix enzyme ornithine transcarbamoylase (OTC) (>3-fold spectral counts for BirA*-ClpP versus BirA*-OTC; Figure 4A; Table S2). The proteins interacting with WT and mutant ClpP were similar. ClpX, the known regulatory subunit of ClpP, was the top hit in our interactome map. Most of the 48 other preferential ClpP-interacting proteins were components of the respiratory chain or enzymes involved in mitochondrial metabolism. Therefore, these data suggested that ClpP function could be important to maintain the integrity of mitochondrial metabolism.

Inhibition of ClpP Impairs Oxidative Phosphorylation

Given the interactions of ClpP with respiratory chain proteins and metabolic enzymes, we evaluated the effects of ClpP inhibition on oxidative phosphorylation. We found that knockdown of ClpP reduced basal oxygen consumption in OCI-AML2 cells (Figure 4B).

Succinate dehydrogenase subunit A (SDHA), a subunit of respiratory chain complex II, was a top hit in our interaction mapping experiment. Therefore, we also measured the effects of ClpP inhibition on the activity of respiratory chain complex II. Knockdown of ClpP reduced the enzymatic activity of complex II in OCI-AML2 cells (Figure 4C). Consistent with impaired complex II activity, knockdown of ClpP also increased mitochondrial reactive oxygen species (ROS) production (Figure 4D). Using non-denaturing gels and immunoblotting, we also observed faster migrating bands of SDHA after ClpP knockdown, potentially representing the accumulation of non-functional misfolded or degraded SDHA (Figure 4E).

To determine whether the changes in oxidative phosphorylation were functionally important for cell death after ClpP inhibition, we examined the impact of ClpP inhibition in Rho (0) cells that lack mitochondrial DNA and oxidative phosphorylation. We knocked down ClpP in WT and Rho (0) 143B cells that expressed similar levels of ClpP protein (Figures 4F–4H). ClpP knockdown reduced the growth and viability of WT 143B cells but had less effect on the growth and viability of Rho (0) cells (Figure 4I). In addition, we evaluated the impact of knocking down SDHA in OCI-AML2 cells. Knockdown of SDHA impaired complex II activity and reduced the growth and viability in these cells (Figures S3A–S3C). Therefore, these results support SDHA as a functionally important substrate for ClpP and a role for ClpP in maintaining oxidative phosphorylation in a subset of AML cells.

Loss of cell viability was not associated with changes in the mtUPR markers Hsp70 or CPN60 or changes in mitochondrial mass or structure in AML cell lines (Figures S3D–S3H).

A Small-Molecule ClpP Inhibitor Is Cytotoxic to AML Cells

Recently, β-lactone inhibitors of bacterial ClpP were developed and shown to be toxic to several bacterial species (Zeiler et al., 2012). As a chemical approach to evaluate the effects of ClpP inhibition on AML and normal cells, we synthesized the

reported bacterial ClpP inhibitor (3RS,4RS)-3-(non-8-en-1-yl)-4-(2-(pyridin-3-yl)ethyl)oxetan-2-one (A2-32-01) (Figure S4A). A2-32-01 inhibited the enzymatic activity of recombinant bacterial ClpP similarly as the activity of the β-lactone inhibitors in the initial study (Zeiler et al., 2012; Figure S4B) as well as the enzymatic activity of recombinant human mitochondrial ClpP (Figure 5A). In addition, A2-32-01 inhibited cleavage of ClpP fluorogenic peptide substrates when added to lysates of mitochondria isolated from AML cells or intact AML cells (Figure 5B). A2-32-01 did not inhibit cytoplasmic chymotrypsin, trypsin, or caspase-like protease enzymatic activity when added to lysates of red blood cells that contained proteasome complexes but lacked mitochondria, therefore demonstrating its specificity for mitochondrial proteases (Figure S4C).

A2-32-01 induced cell death in TEX, OCI-AML2, and K562 leukemia cells at concentrations that matched its ability to inhibit ClpP activity, but was not toxic to HL60 leukemia cells, which express much lower levels of ClpP (Figures 5C and 5D). However, HL60 cells were more sensitive to the proteasome inhibitor bortezomib (Figure S4D). Similar to ClpP shRNA, A2-32-01 reduced the growth and viability of WT 143B cells but had little effect on the growth and viability of their Rho (0) counterparts (Figure 5E). Moreover, addition of A2-32-01 to OCI-AML2 cells produced no additional loss of growth and viability after knockdown of ClpP (Figure S4E). We also evaluated analogs of A2-32-01. The related compound A2-58-06 had activity similar to A2-32-01, whereas A2-54-01 did not inhibit ClpP and did not reduce the growth and viability of TEX and OCI-AML2 cells (Figures S4F and S4G).

Although A2-32-01 was stable in DMSO, it was rapidly hydrolyzed when dissolved in cell culture medium, with >90% of the compound degraded within 1 hr (Figure S4H). We confirmed that degradation products were inactive (data not shown). This rapid degradation likely explains the high half-maximal inhibitory concentration (IC_{50}) of the compound.

Next we assessed the impact of A2-32-01 on primary AML and normal hematopoietic cells. A2-32-01 showed significant dose-dependent killing of primary AML patient cells that expressed elevated levels of ClpP. In contrast, the same treatment had little effect on either normal hematopoietic cells or primary AML cells that expressed lower levels of ClpP (Figures 6A–6C). In fact, primary AML cells showed a strong positive correlation between ClpP expression and sensitivity to A2-32-01 (Figure 6D). Therefore, ClpP expression might serve as a biomarker for patients who would respond to ClpP inhibitors.

A2-32-01 Shows Anti-AML Activity in Xenograft Models of Human Leukemia

Finally, we evaluated the anti-leukemia efficacy and toxicity of A2-32-01 in mouse models of leukemia. Dissolving A2-32-01 in corn oil preserved its stability while in solution, and the pharmacokinetics of A2-32-01 were determined after intraperitoneal (i.p.) injection of the compound into SCID mice (Figures S5A and S5B). Next, we evaluated the efficacy and toxicity of A2-32-01 in mice xenografted with OCI-AML2 cells. Daily treatment with A2-32-01 delayed the growth of OCI-AML2 cells in SCID mice without evidence of liver, muscle, or renal toxicity (Figure 7A; Figures S5C and S5D). Moreover, tumors excised from mice treated for 5 days with A2-32-01 had reduced respiratory chain complex II activity compared with vehicle-treated controls (Figure 7B) and reduced enzymatic activity of ClpP (Figure 7C). Therefore, A2-32-01 inhibits growth and mitochondrial function of this AML cell line in vivo.

We also assessed the efficacy and toxicity of A2-32-01 in NOD-SCID mice engrafted intra-femorally with primary AML cells. A2-32-01 treated mice had significantly lower levels of leukemic engraftment compared to control-treated mice without evidence of toxicity (Figure 7D). Thus, inhibiting ClpP may be an effective strategy for a subset of AML patients.

DISCUSSION

The therapy for AML has remained largely unchanged over the last 20 years, and the outcome for most patients is poor. In search of more effective approaches, we found recently that blocking mitochondrial protein translation was selectively cytotoxic to AML cells (Skrtić et al., 2011). This followed the discovery that a subset of AML cells have unique mitochondrial characteristics with increased mitochondrial biogenesis and increased reliance on oxidative phosphorylation that could be inhibited by targeting mitochondrial protein translation (Lagadinou et al., 2013; Skrtić et al., 2011). Here we identify ClpP as a potential component of the mitochondrial proteome whose inhibition might be cytotoxic to AML cells. We found that ClpP is overexpressed in leukemic cells from a group of AML patients and that inhibition of ClpP selectively induces death in these cells without apparent toxicity to normal hematopoiesis. The fact that increased expression of ClpP occurs across all currently defined subtypes of AML based on their morphologic, cytogenetic, or mutational features, including those with a poor prognosis, lends further support to the possibility that ClpP may be an important therapeutic target for the treatment of AML. In addition, ClpP expression may be a useful biomarker to identify patients most likely to respond to ClpP inhibitors.

Little is known about the endogenous proteins that interact with ClpP in the mitochondria of mammalian cells. Here we identified that most of the proteins interacted with ClpP were components of the respiratory chain and mitochondrial metabolic enzymes. It is noteworthy that a similar set of ClpP substrates, including the respiratory chain complex component SDHA, were identified by Haynes et al. (2010) in their studies of ClpP function in *C. elegans*. Therefore, ClpP appears to function to maintain the integrity of the respiratory chain and mitochondrial metabolism.

In *C. elegans*, peptides generated by ClpP-mediated protein degradation are exported from the mitochondria via the transporter haf-1 and signal the mtUPR response in the nucleus (Haynes et al., 2007, 2010). Upon mitochondrial stress, levels of ClpP and mtUPR-associated genes increase. To date, the mechanisms by which ClpP regulates the mtUPR in mammalian cells remain unknown, and the mammalian homolog of haf-1 has not yet been defined.

In our study, gene expression analysis demonstrated that higher levels of ClpP were associated with greater expression of genes associated with the mtUPR. Because of increased mitochondrial mass, high metabolic and biosynthetic requirements, and imbalances between levels of nuclear and mitochondrial encoded proteins, we hypothesize that the mitochondria in a subset of AML and other cancer cells are under increased

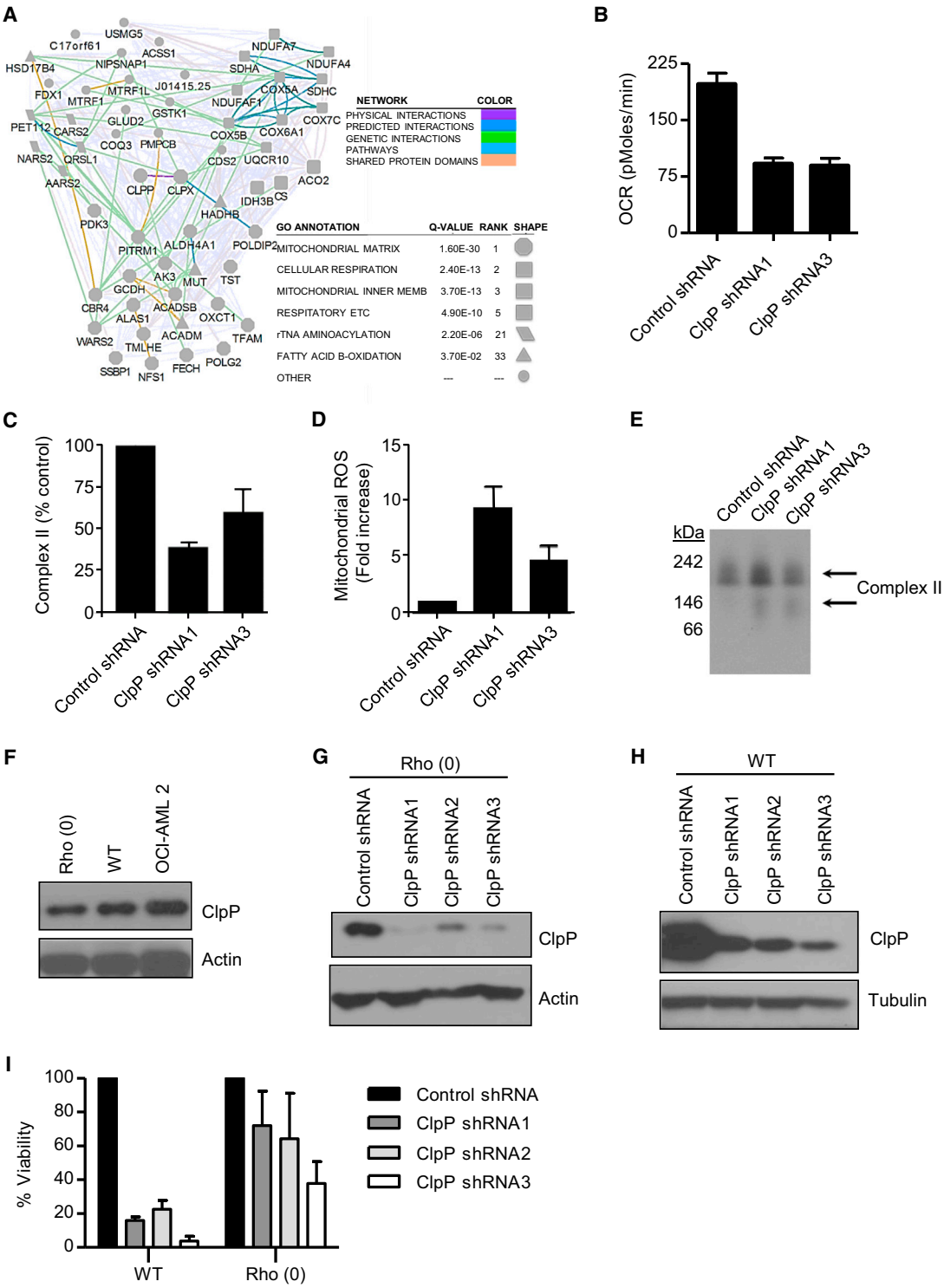

Figure 4. ClpP Regulates Mitochondrial Metabolism

(A) Network of proteins that interacted with WT or catalytically inactive ClpP.

(B) Effects of ClpP knockdown on basal oxygen consumption (OCR) in OCI-AML2 cells 4 days after transduction with ClpP shRNA or control sequences. Mean ± SD cell counts from one of three representative experiments are shown.

(C) Effects of ClpP knockdown on complex II activity in OCI-AML2 cells 4 days after transduction with ClpP shRNA or control sequences. The percent mean ± SD enzymatic activity from one of three representative experiments is shown.

(D) Effects of ClpP knockdown on mitochondrial ROS production in OCI-AML2 cells 4 days after transduction with ClpP shRNA or control sequences. Mean ± SD mitochondrial ROS-positive cells from one of three representative experiments are shown.

(legend continued on next page)

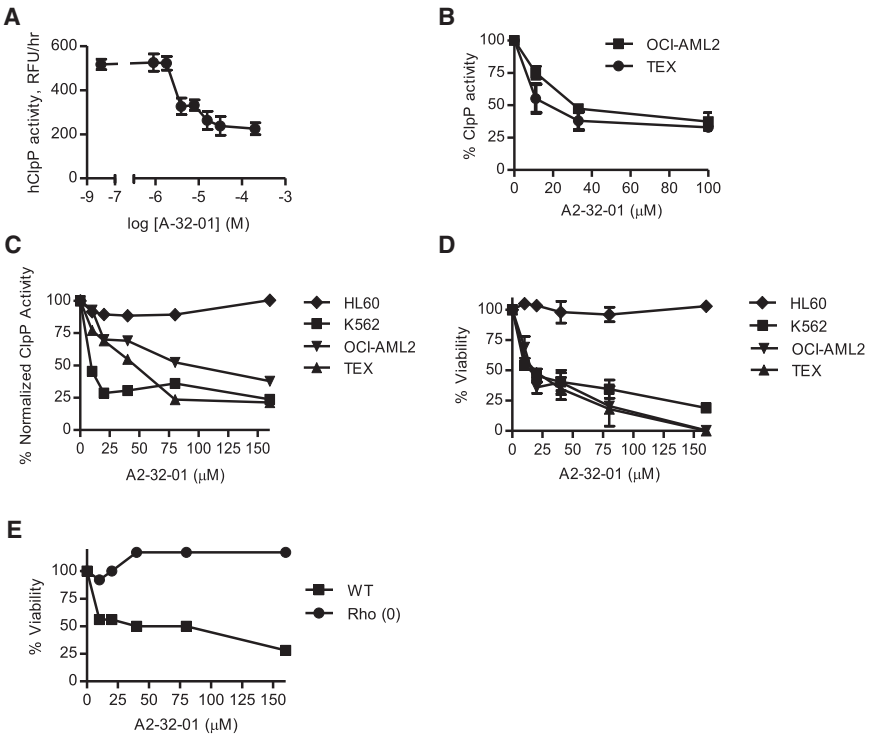

Figure 5. A2-32-01 Inhibits ClpP and Is Cytotoxic to AML Cells

(A) Effect of A2-32-01 on the ability of recombinant human ClpP and ClpX to cleave the fluorogenic substrate casein-FITC (mean ± SD). RFU, relative fluorescence unit.

(B) Effect of A2-32-01 on ClpP activity measured in mitochondrial lysates from OCI-AML2 and TEX cells after 2 hr based on cleavage of the fluorogenic substrate Suc-LY-AMC (percent mean ± SD).

(C) Effect of 48-hr A2-32-01 treatment on the activity of ClpP in HL60, K562, OCI-AML2, and TEX cells based on the cleavage of the fluorogenic substrate Suc-LY-AMC. Normalized data are shown.

(D) Effect of 48-hr A2-32-01 treatment on the viability of HL60, K562, OCI-AML2, and TEX cells. The percent mean ± SD of viable cells was measured by trypan blue staining.

(E) Effect of 48-hr A2-32-01 treatment on the viability of WT and Rho (0) 143B cells. The percent of viable cells was measured by trypan blue staining.

See also Figure S4.

basal stress and have upregulated ClpP in response to these stressors. In support of this hypothesis, induction of mitochondrial protein aggregates through the overexpression of mutant OTC in COS-7 cells induced mtUPR and increased ClpP expression (Zhao et al., 2002).

Mechanisms that regulate ClpP expression in AML cells are unknown and are an important direction for future study. In COS-7 cells, the expression of ClpP may be regulated at the level of its promoter by a combination of CHOP, MURE1, and MURE2 sequences (Aldridge et al., 2007). However, it is unknown whether these sequences also regulate ClpP expression in AML cells, and the transcription factors that bind these sites are unknown. In addition, regulation of ClpP may also occur at the level of protein translation and degradation.

We used the bacterial ClpP inhibitor A2-32-01 to examine the impact of inhibiting mitochondrial ClpP in AML because the compound cross-reacted with the mitochondrial isoform. However, it is important to note that the selectivity of A2-32-01 for mitochondrial ClpP over other mammalian targets, including other mitochondrial proteases, remains to be determined. In addition, A2-32-301 has poor stability in aqueous media, so this molecule would not have therapeutic applications, and its ability to reduce large bulk disease may be limited. Developing potent, stable, and specific ClpP inhibitors based on alternate scaffolds is a priority to fully assess the efficacy and toxicity of ClpP inhibition in vivo.

In AML cells, loss of viability after inhibition of ClpP was associated with impairment of mitochondrial metabolism and oxidative phosphorylation. This finding is consistent with prior studies demonstrating that AML cells and stem cells have an increased reliance on oxidative phosphorylation (Skrtić et al., 2011; Lagadinou et al., 2013). The fact that elevated ClpP expression was not associated with any known molecular or clinical feature of AML is consistent with this variable phenotype and suggests that increased ClpP expression may be a consequence of multiple dysregulated pathways that converge to impact mitochondrial function and metabolism.

In addition to ClpP, our shRNA screen of the mitochondrial proteome identified three other mitochondrial proteases whose knockdown reduced the growth and viability of K562 cells (NLN, PARL, and PITRM1). Little is known about mitochondrial proteases as cancer targets and the impact of inhibiting select mitochondrial proteases in malignant cells. Potentially, these proteases could also be important therapeutic targets for AML given their role in regulating mitochondrial function. For example, PARL regulates PINK1 turnover, and knockdown of PARL promotes accumulation of PINK1 on the mitochondrial surface, leading to increased mitophagy (Greene et al., 2012). However, further studies will be

(E) Effect of ClpP knockdown in OCI-AML2 cells 4 days after infection with virus expressing shRNA targeting ClpP or control sequences on SDHA expression and migration on a native gel determined by immunoblotting.

(F) Expression of ClpP in total cell lysates prepared from WT and Rho (0) 143B and OCI-AML2 cells.

(G and H) The expression of ClpP and β-actin were detected by immunoblotting in WT (G) and Rho (0) 143B (H) cells transduced with individual shRNA targeting ClpP or control sequences.

(I) The number of viable WT and Rho (0) 143B cells was measured by trypan blue staining 12 days after transduction as described in (F) and (G). One of three representative experiments showing the percent mean ± SD viable cells relative to cells infected with control shRNA is presented.

See also Figure S3 and Table S2.

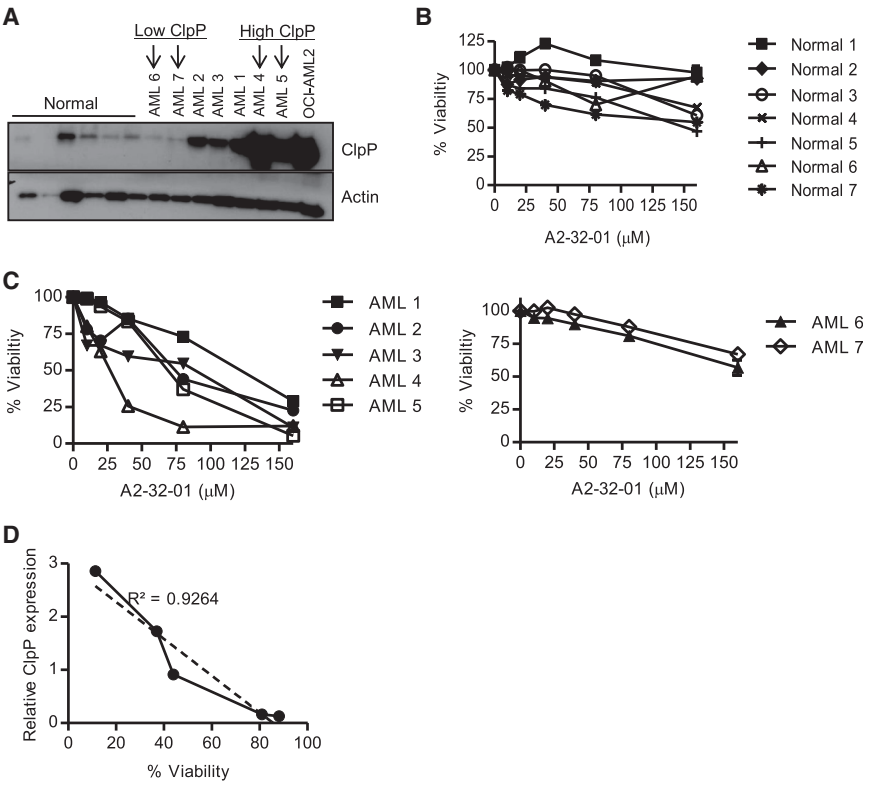

Figure 6. ClpP Expression Correlates with Sensitivity to A2-32-01 in Primary AML Cells

(A) Expression of ClpP and Actin in primary normal hematopoietic cells, primary AML patient samples, and OCI-AML2 cells was determined by immunoblotting.

(B and C) Effect of A2-32-01 on the viability of primary normal hematopoietic cells (B) and primary AML cells (C) assessed after a 48-hr period of exposure. The mean ± SD percent of viable cells was measured by Annexin V/propidium iodide (PI) staining and flow cytometry.

(D) Correlation analysis of ClpP expression and cell viability of primary AML cells. Cell viability was measured by Annexin-V/PI staining 48 hr after treatment with 80 μM of A2-32-01.

necessary to fully understand the efficacy and toxicity of inhibiting PARL and other mitochondrial proteases in vitro and in vivo.

Therefore, in summary, although AML may have significant molecular and genetic heterogeneity, the dysregulation of some biological pathways such as mitochondrial function and metabolism remain common and may be amenable to therapeutic exploitation.

EXPERIMENTAL PROCEDURES

See Supplemental Experimental Procedures for additional experimental procedures.

shRNA Screen to Identify Targets in the Mitochondrial Proteome

To identify shRNA that reduced the growth and viability of AML cells, we performed a pooled lentiviral shRNA screen in K562 cells similar to one described previously (Ketela et al., 2011). K562 cells were selected because of their robust transduction efficiencies, and their reliance on BCR-ABL1 signaling served as a positive control for the screen. K562 leukemia cells were transduced with a pooled lentiviral library consisting of 54,021 shRNAs in barcoded lentiviral vectors with puromycin selection markers targeting 11,255 nuclearly encoded genes. Of these, 34,600 were associated with known genes and transcripts. These sequences were considered in the analysis. Cells were transduced at a multiplicity of infection of 0.3, ensuring that each cell receives at most one shRNA. The day after infection, cells were treated with puromycin to select infected cells. Resistant clones, containing a lentiviral vector and its associated shRNA, were then grown in puromycin-containing medium for 21 days. After 21 days, cells were harvested, genomic DNA was isolated, and the abundance of barcoded sequences was identified by microarray analysis. In conducting our lentiviral shRNA, we performed two independent experiments utilizing the same amount of virus for transduction (inter-experiment or biological replicates). Each trial was analyzed in duplicate on arrays (intra-experiment or technical replicates), leading to the generation of four replicates (two biological and two technical) for the 0- and 21-day time points.

Log_2 background-corrected fluorescence signal intensities were compared pairwise for all intra- and inter-experimental replicates at 0 and 21 days to ensure technical and experimental reproducibility. Correlation coefficients for all pairwise comparisons were $r^2 > 0.97$. Therefore, all four technical and experimental replicates for each time point were averaged to compare the 0- and 21-day time points. Fold changes were computed by calculating the difference in mean Log_2 (background-corrected fluorescence signal intensities) for each individual shRNA as follows:

$$Log_2(\text{fold-change}) = Log_2(\text{mean intensity}_{t=21\ \text{days}}) - Log_2(\text{mean intensity}_{t=0\ \text{days}}).$$

Negative values indicated potential depletion of the individual shRNA. A percent depletion value was also calculated as follows: % depletion = $(1-2^{Log_2(\text{fold-change})}) \times 100\%$.

shRNAs in the screen were ranked based on Log_2(fold change) and percent depletion values. shRNAs were also grouped by target gene to assess whether multiple shRNAs targeting the same gene had high percent depletion scores. Genes encoding the mitochondrial proteome were identified using MitoCarta (http://www.broadinstitute.org/pubs/MitoCarta/).

Reverse-Phase Protein Array

A reverse phase protein array (RPPA) was generated by using samples from patients with AML, myelodysplastic syndrome (MDS), and normal $CD34^+$ cells as described previously (Kornblau and Coombes, 2011; Kornblau et al., 2010, 2011; Pierce et al., 2013; Tibes et al., 2006). The ClpP antibody was validated for use in the RPPA assay as described previously (Kornblau and Coombes, 2011; Kornblau et al., 2010, 2011; Pierce et al., 2013; Tibes et al., 2006). Briefly, the rabbit monoclonal ClpP antibody (clone ab124822, Abcam) was validated to recognize only a single band corresponding to the expected molecular weight by immunoblotting. In addition, the sensitivity of the antibody in the RPPA assay was validated using an array of cell line lysates seeded in serials dilutions. The RPPA signal was linear over the range of dilutions. In addition, the signal obtained with cell lysate dilutions by RPPA correlated with the signal intensity by observed by immunoblotting ($R^2 = 0.75$). When the RPPA was optimized for detection of ClpP expression, patient and normal samples were printed in five serial dilutions onto slides along with normalization and expression controls. Slides were probed with anti-ClpP primary antibody (Abcam, catalog no. 124822) at 1:1,000 and a secondary antibody followed by colorimetric assay. Stained slides were analyzed using Microvigene software (Vigene Tech).

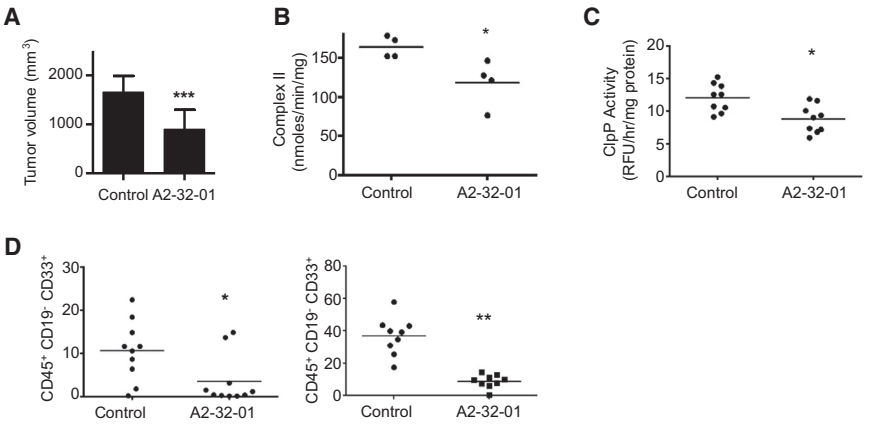

Figure 7. A2-32-01 Shows Anti-AML Activity in Xenograft Models of Human Leukemia

(A) Effect of i.p. injection of 300 mg/kg of A2-32-01 or corn oil vehicle control twice daily for 5 of 7 days on tumor volume when OCI-AML2 cells were xenografted into SCID mice (n = 10 mice/group). Mean ± SD, ***p < 0.001 by t test.

(B) Respiratory chain complex II activity in tumors from SCID mice xenografted with OCI-AML2 cells and treated with i.p. injection of 300 mg/kg A2-32-01 or corn oil vehicle control daily for 5 days (n = 4 mice/group). *p = 0.03 by t test. Horizontal bars indicate the mean.

(C) ClpP activity measured by the cleavage of the fluorogenic substrate casein-FITC in mitochondrial lysates in tumors from SCID mice xenografted with OCI-AML2 cells and treated with i.p. injection of 300 mg/kg A2-32-01 or corn oil vehicle control daily for 4 days (n = 9 mice/group). *p = 0.005 by t test. Horizontal bars indicate the mean.

(D) Human leukemia cell engraftment in sublethally irradiated female NOD/SCID mice and treated with A2-32-01 (300 mg/kg by i.p. injection daily) or vehicle control (n = 10 mice/group) 3 of 7 days for 4 weeks was measured by flow cytometric analysis. Shown are results from two independent experiments. *p = 0.02 and **p < 0.0001 by t test. Horizontal bars indicate the mean.

See also Figure S5.

Primary AML and Normal Hematopoietic Cells

Primary mononuclear cells were isolated from peripheral blood samples from consenting patients with AML whose blast count was 80% or higher by low-density cells isolated by Ficoll density centrifugation. Granulocyte colony-stimulating factor (G-CSF)-mobilized peripheral blood stem cells were obtained from healthy consenting volunteers donating peripheral blood stem cells for allogeneic stem cell transplantation. All primary cells were cultured at 37°C in Iscove's modified Dulbecco's medium (IMDM) supplemented with 20% fetal bovine serum (FBS) and penicillin-streptomycin. Informed consent was obtained from all subjects for the collection and use of samples. The collection and use of human tissue for this study were approved by the University Health Network Institutional Review Board and Review Ethics Board of the University of British Columbia.

shRNA Knockdown of ClpP

Construction of hairpin-pLKO.1 vectors (carrying a puromycin antibiotic resistance gene) containing shRNA sequences and production of shRNA viruses was performed as described previously (Simpson et al., 2012). The shRNAs targeting the ClpP (accession no. NM_003321) coding sequence are as follows: ClpP shRNA1, 5′-GCCCATCCACATGTACATCAA-3′; ClpP shRNA2, 5′-CACGATGCAGTACATCCTCAA−3′; and ClpP shRNA3, 5′-GCTCAAGAAGCAGCTCTATAA−3′.

Lentiviral transduction was performed essentially as described previously (Xu et al., 2010). Briefly, cells (5 × 10^6) were centrifuged and resuspended in 5 ml of medium containing protamine sulfate (5 μg/ml). 0.5 ml of virus (for adherent cells) and 2 ml of virus (for suspension cells) were added to the cells, followed by overnight incubation (37°C, 5% CO_2). Cells were centrifuged and washed, and fresh medium with puromycin (1μg/ml) was added the following day. Three days later, cells were cultured to measure viability and growth.

Equal numbers of TEX cells transduced with shRNA targeting ClpP or control sequences (2 × 10^5) were injected into the right femur of sublethally irradiated NOD/SCID-GF mice with human transgenes producing interleukin-3 (IL-3), granulocyte/macrophage-stimulating factor (GM-CSF), and Steel factor (SF) (n = 10/group) (Nicolini et al., 2004). 6 weeks after injection, mice were sacrificed, and the percentage of human $CD45^+$ cells in the non-injected left femur was determined by flow cytometry.

Evaluation of Hematopoietic Progenitors in WT and *Clpp*$^{-/-}$ Mice

Heterozygous *Clpp* knockout mice (C57BL/6N background) were obtained from the Texas A&M Institute for Genomic Medicine, and breeding pairs were established in our facility. Studies with *Clpp* $^{-/-}$ mice were carried out according to the regulations of the Canadian Council on Animal Care and with the approval of the Ontario Cancer Institute and BC Cancer Agency animal ethics review boards.

Hematopoietic cells were flushed from the femora and tibiae of *Clpp*$^{+/+}$ and *Clpp* $^{-/-}$ mice using DMEM and 2% fetal calf serum (FCS) and passed through a 70 μM strainer. The population was enriched for lineage-negative (Lin^-) progenitor cells using magnetic bead separation (lineage cell depletion kit, Miltenyi). Cells (1-2 × 10^6) were preincubated with an Fc block for 10 min at 4°C and immunostained with antibodies recognizing Sca1 (D7) and cKit (2B8) (both from eBioscience). Flow cytometry data were acquired using a FACSCanto II (BD Biosciences) flow cytometer and analyzed with the FlowJo analysis program.

W^{41}/*W*^{41} CD45.1 sublethally irradiated (400 rad) mice were transplanted with 10^6 CD45.2 hematopoietic cells from the femora of WT or *Clpp* $^{-/-}$ mice along with 10^6 competitor CD45.1 hematopoietic cells. Cells from two *Clpp*$^{+/+}$ WT mice were pooled and injected into five recipient CD45.1 mice. Cells from each of three *Clpp* $^{-/-}$ mice were injected into four to six CD45.1 recipients. Peripheral blood samples were collected from the tail vein of recipient mice 5, 8, and 12 weeks after transplantation. Following lysis of the red blood cells with ammonium chloride (StemCell), the white blood cells (WBCs) were stained with antibodies for donor and recipient CD0.45 allotypes: anti-CD45.1-PECy7 (eBioscience) and anti-CD45.2-APCef780 (eBioscience) plus $CD19^-$BV421 (BioLegend) for B cells, Ly6G-PE and Mac-1-PE (both BD Pharmingen) for myeloid cells, and CD3e-APC (BioLegend) for T cells. To calculate repopulation levels, the contributions of the donor CD45.2-positive cells to the populations of circulating GM, B, and T cells and total WBCs were calculated.

To examine T cell function in *Clpp* $^{-/-}$ and *Clpp*$^{+/+}$ mice, 5 × 10^6 splenocytes/well were seeded in wells coated with 3 μg/ml hamster anti-mouse CD3 (clone 2C11-145, BD Biosciences) and 1 μg/ml hamster anti-mouse CD28 (clone 37.51, eBioscience) for 24 hr. For B cell activation, splenocytes (5 × 10^6/well) were cultured for 24 hr with 10 μg/ml goat anti-mouse immunoglobulin M (IgM) (F(ab')2 fragment, Jackson ImmunoResearch). To assess activation status, cells were stained with fluorescence-conjugated antibodies against surface markers. Flow cytometry data were acquired using a FACSCanto II (BD Biosciences) flow cytometer and analyzed with the FlowJo analysis program.

BioID-MS to Identify ClpP-Interacting Proteins

Stable 293 T-REx cell pools expressing tetracycline-regulated, BirA*-tagged WT, or catalytically inactive mutant ClpP proteins were generated. Cell pools expressing the BirA* epitope tag alone or BirA* fused to the unrelated mitochondrial enzyme OTC were also created for use as negative controls. 293 T-REx cells (at ~60% confluence) were treated with 1 μg/ml tetracycline and 50 μM biotin for 24 hr to induce transgene expression and effect biotinylation of nearby polypeptides. Cells were scraped into PBS, pooled, washed twice in 25 ml PBS, and collected by centrifugation at 1000 × *g* for 5 min at 4°C. Cell pellets were lysed in 5 ml ice-cold modified RIPA buffer. 250 U benzonase

(EMD Millipore) was added, and biotinylated proteins were isolated. The resulting supernatant was incubated with 30 μl of (RIPA-equilibrated) streptavidin-Sepharose beads (GE Healthcare) with end-over-end rotation for 2 hr at 4°C. Beads were washed seven times with 1 ml of 50 mM ammonium bicarbonate (pH 8.0) prior to tryptic digestion.

Mass Spectrometry to Identify ClpP-Interacting Proteins

One microgram of MS-grade L-(tosylamido-2-phenyl) ethyl chloromethyl ketone (TPCK) trypsin (Promega) dissolved in 70 μl of 50 mM ammonium bicarbonate (pH 8.3) was added to the streptavidin-Sepharose beads and incubated at 37°C overnight. The eluate was collected, and beads were washed twice in 100 μl of 50 mM ammonium bicarbonate. The combined eluate was lyophilized and then resuspended in 0.1% formic acid. Liquid chromatography (LC) analytical columns (75-μm inner diameter) and pre-columns (150-μm inner diameter) were made in-house from fused silica capillary tubing from InnovaQuartz and packed with 100 Å C18-coated silica particles (Magic, Michrom Bioresources). Peptides were subjected to nano liquid chromatography-electrospray ionization-tandem mass spectrometry (LC-ESI-MS/MS) using a 95-min reverse-phase (10%–30% acetonitrile, 0.1% formic acid) buffer gradient running at 250 nl/min on a Proxeon EASY-nLC pump in-line with a hybrid linear quadrupole ion trap (Velos LTQ) Orbitrap mass spectrometer (Thermo Fisher Scientific). A parent ion scan was performed in the Orbitrap using a resolving power of 60,000. Simultaneously, the 20 most intense peaks were selected for MS/MS (minimum ion count of 1,000 for activation) using standard collision-induced dissociation (CID) fragmentation. Fragment ions were detected in the LTQ. Dynamic exclusion was activated so that MS/MS of the same mass to charge ratio (m/z) (within a 10-ppm window, exclusion list size 500) detected two times within 15 s were excluded from analysis for 30 s.

For protein identification, Thermo.RAW files were converted to the .mzXML format using Proteowizard as part of the trans-proteomic pipeline (Keller and Shteynberg, 2011). For each search, the iProphet probability at a 1% error rate was used as a cutoff value to generate statistical analysis of interactomes (SAINT)-compatible input files. SAINT parameters were as follows: 5,000 iterations, low mode off, minFold 1, and normalization on Choi et al., 2011).

Via the ProHits suite (Liu et al., 2010, 2012), MS data were analyzed using the X!Tandem database search algorithm, and the resulting peptide identifications were subjected to iProphet analysis (Shteynberg et al., 2011) within the trans-proteomic pipeline (Keller and Shteynberg, 2011). Using BirA*-only cell data as a control for endogenous biotinylated proteins and polypeptides that interact non-specifically with the solid phase support, the BirA*-ClpP data were subjected to SAINT (Choi et al., 2011) to identify bona fide interacting partners. Polypeptides identified with an iProphet confidence value of >0.8 (reflecting an ~1% error rate) and assigned a maximum SAINT confidence value of >0.80 are shown in Figure S3A.

The network of proteins that interacted with WT or catalytically inactive ClpP preferentially over OTC or empty vector were defined using GeneMANIA 3.3.1, Cytoscape 3.1.0 (Montojo et al., 2010). Preferential interactions compared with OTC or empty vector were identified in 293 T-REx cells using the BirA* tagging method.

Bacterial and Human ClpP Activity

Bacterial ClpP was purified from *E. coli* as described previously (Kimber et al., 2010). To measure ClpP peptidase activity, 1 μM ClpP (monomer concentration) was dissolved in assay buffer (50 mM Tris-Cl [pH 8.0], 200 mM KCl, and 1 mM DTT) with 0.5 mM succinyl-leucine-tyrosine-7-amino-4-methylcoumarin (Suc-LY-AMC). This mixture was then plated at 50 μl/well in a 96-well plate and read for fluorescence at 2-min intervals for 1 hr at 360/460 nm. The rate of ClpP was determined by calculating the slope (in the linear range).

Human recombinant ClpP (1.2 μM) and ClpX (1.0 μM) were combined and dissolved in assay buffer consisting of 25 mM N-2-hydroxyethylpiperazine-N'-2-ethanesulfonic acid (HEPES) (pH 7.5), 5 mM $MgCl_2$, 5 mM KCl, 0.03% Tween 20, and 10% glycerol with an ATP regeneration system of 16 mM creatine phosphate and 13 U/ml creatine kinase. 3 mM ATP was added along with the ClpX substrate, casein-fluorescein isothiocyanate (FITC, 4.5 μM). All components were mixed and covered from light at 37°C for 5 min. The mixture was then plated at 200 μl/well in triplicates in a 96-well plate with or without ClpP inhibitors. Fluorescence at 485/535 nm was measured at 37°C every 10 min for 6 hr. The rate of ClpP activity was determined by calculating the slope (in the linear range).

Purification of Human ClpP and ClpX

Plasmids encoding human ClpP and ClpX were transformed into B21 Gold DE3 pLys and B21 Gold DE3 bacteria, respectively. Transformed bacteria were plated on Luria broth (LB)-agar plates containing 100 μg/ml ampicillin and incubated overnight at 37°C. The following day, individual colonies were grown overnight at 37°C in LB medium containing 100 μg/ml ampicillin (ClpP) or 85 μg/ml chloramphenicol and 100 μg/ml ampicillin (ClpX). ClpP and ClpX expression were induced with 1 mM isopropyl β-D-1-thiogalactopyranoside (IPTG) in Terrific medium without antibiotics. Bacteria were collected after 4 hr, and the pellet was frozen at −70°C. ClpP and ClpX proteins were purified on Ni-agarose using lysis buffer (25 mM Tris-HCl [pH 7.5], 500 mM NaCl, 10% Glycerol, 5 mM mercaptoethanol, and 10 mM imidazole), wash buffer (25 mM Tris-HCl [pH 7.5], 500 mM NaCl, 10% Glycerol, 5 mM mercaptoethanol, and 50 mM imidazole), and elution buffer (25 mM Tris-HCl [pH 7.5], 500 mM NaCl, 10% Glycerol, 5 mM mercaptoethanol, and 250 mM imidazole). The proteins were dialyzed for 4 hr at 4°C in dialysis buffer (50 mM Tris-HCl [pH 7.5], 200 mM KCl, 25mM $MgCl_2$, 10% g1ycerol, 1 mM DTT, and 0.1 mM EDTA). The recombinant proteins were stored at −70°C.

ClpP Activity in Isolated Mitochondria

Intact mitochondria from cell lines were isolated as described above. The fluorogenic substrate Suc-LY-AMC (0.5 mM) was added to mitochondrial lysates in ClpP peptidase assay buffer (50 mM Tris-Cl [pH 8.0], 200 mM KCl, 1 mM DTT, 0.1% n-dodecyl β-D-maltoside [DDM], and 2 mM ATP). This mixture was plated at 50 μl/well in a 96-well plate, and fluorescence was measured at 2-min intervals for 1 hr (360/460nm). The rate of ClpP activity was determined by calculating the slope (in the linear range).

Assessment of Anti-Leukemia Activity of A2-32-01 in Mouse Models of Human Leukemia

OCI-AML2 human leukemia cells (5×10^5) were injected subcutaneously into the flanks of male SCID mice (Ontario Cancer Institute). When the tumors were palpable, mice were treated with A2-32-01 or vehicle control (corn oil) by i.p. injection (300 mg/kg twice daily for 5 of 7 days) for 10 days (n = 10/group). Tumor volume was measured using caliper measurements at the end of the experiment. Mice were sacrificed, and organs were harvested, fixed with 10% buffered formalin, embedded, sectioned, and stained with H&E. The stained samples were scanned using Aperio Scanscope XT at 10× magnification and analyzed using Aperio ImageScope.

To assess the effect of A2-32-01 on complex II activity in vivo, OCI-AML2 human leukemia cells (5×10^5) were injected subcutaneously into the flanks of male SCID mice (Ontario Cancer Institute). When the tumors were palpable, mice were treated with A2-32-01 or vehicle control (corn oil) by i.p. injection (300 mg/kg daily) for 5 days (n = 4/group). After 5 days, tumors were excised, and complex II activity was measured as above.

To assess A2-32-01 in mouse models of primary AML engraftment, a frozen aliquot of AML cells was thawed, counted, and re-suspended in PBS, and 2.5×10^6 viable trypan blue-negative cells were injected into the right femur of 10 week-old female NOD-SCID mice that had been irradiated 24 hr previously with 208 rad from a ^{137}Cs source and injected with 200 μg anti-mouse CD122. Two weeks after injection of AML cells, mice were treated with A2-32-01 (300 mg/kg by i.p. injection) or vehicle control (n = 10/group) 3 of 7 days for 4 weeks. Mice were then sacrificed, and the cells were flushed from the femora. Engraftment of human AML cells into the marrow of the non-injected left femur was assessed by enumerating the percentage of human $CD45^+CD33^+CD19^-$ cells by flow cytometry using the BD Biosciences FACSCalibur. Data were analyzed with FlowJo version 7.7.1 (Tree Star).

All animal studies were carried out according to the regulations of the Canadian Council on Animal Care and with the approval of the Ontario Cancer Institute animal ethics review board.

ACCESSION NUMBERS

The microarray data from the screen were deposited with the following accession number: GenomeRNAi: GR00343-S.

SUPPLEMENTAL INFORMATION

Supplemental Information includes Supplemental Experimental Procedures, five figures, and two tables and can be found with this article online at http://dx.doi.org/10.1016/j.ccell.2015.05.004.

ACKNOWLEDGMENTS

We thank Urlich Baxa (Electron Microscopy Laboratory, NCI [NIH]) for help with electron microscopy, Aisha Shamas-Din (Princess Margaret Cancer Centre) for help with preparing the manuscript, and Jill Flewelling (Princess Margaret Cancer Centre) for administrative assistance. This work was supported by the Canadian Stem Cell Network, the Leukemia and Lymphoma Society, the NIH (NCI 1R01CA157456), the Canadian Institutes of Health Research, a Terry Fox Research Foundation Program Project Group Grant (to C.J.E.), MaRS Innovation, the Ontario Institute for Cancer Research with funding provided by the Ontario Ministry of Research and Innovation, the Princess Margaret Cancer Centre Foundation, and the Ministry of Long Term Health and Planning in the Province of Ontario. S.B. was supported by a Vanier Scholarship award from CIHR. D.V.J. is a Fonds de recherche du Québec – Santé (FRQS) postdoctoral scholar. A.D.S. holds the Barbara Baker Chair in Leukemia and Related Diseases.

Received: November 4, 2014
Revised: February 6, 2015
Accepted: May 7, 2015
Published: June 8, 2015

REFERENCES

Aldridge, J.E., Horibe, T., and Hoogenraad, N.J. (2007). Discovery of genes activated by the mitochondrial unfolded protein response (mtUPR) and cognate promoter elements. PLoS ONE *2*, e874.

Choi, H., Larsen, B., Lin, Z.Y., Breitkreutz, A., Mellacheruvu, D., Fermin, D., Qin, Z.S., Tyers, M., Gingras, A.C., and Nesvizhskii, A.I. (2011). SAINT: probabilistic scoring of affinity purification-mass spectrometry data. Nat. Methods *8*, 70–73.

Conlon, B.P., Nakayasu, E.S., Fleck, L.E., LaFleur, M.D., Isabella, V.M., Coleman, K., Leonard, S.N., Smith, R.D., Adkins, J.N., and Lewis, K. (2013). Activated ClpP kills persisters and eradicates a chronic biofilm infection. Nature *503*, 365–370.

Corydon, T.J., Bross, P., Holst, H.U., Neve, S., Kristiansen, K., Gregersen, N., and Bolund, L. (1998). A human homologue of Escherichia coli ClpP caseinolytic protease: recombinant expression, intracellular processing and subcellular localization. Biochem. J. *331*, 309–316.

Dan, S., Naito, M., and Tsuruo, T. (1998). Selective induction of apoptosis in Philadelphia chromosome-positive chronic myelogenous leukemia cells by an inhibitor of BCR - ABL tyrosine kinase, CGP 57148. Cell Death Differ. *5*, 710–715.

de Sagarra, M.R., Mayo, I., Marco, S., Rodríguez-Vilariño, S., Oliva, J., Carrascosa, J.L., and Casta ñ, J.G. (1999). Mitochondrial localization and oligomeric structure of HClpP, the human homologue of E. coli ClpP. J. Mol. Biol. *292*, 819–825.

Fisher, R.I., Bernstein, S.H., Kahl, B.S., Djulbegovic, B., Robertson, M.J., de Vos, S., Epner, E., Krishnan, A., Leonard, J.P., Lonial, S., et al. (2006). Multicenter phase II study of bortezomib in patients with relapsed or refractory mantle cell lymphoma. J. Clin. Oncol. *24*, 4867–4874.

Gispert, S., Parganlija, D., Klinkenberg, M., Dröse, S., Wittig, I., Mittelbronn, M., Grzmil, P., Koob, S., Hamann, A., Walter, M., et al. (2013). Loss of mitochondrial peptidase Clpp leads to infertility, hearing loss plus growth retardation via accumulation of CLPX, mtDNA and inflammatory factors. Hum. Mol. Genet. *22*, 4871–4887.

Goard, C.A., and Schimmer, A.D. (2014). Mitochondrial matrix proteases as novel therapeutic targets in malignancy. Oncogene *33*, 2690–2699.

Greene, A.W., Grenier, K., Aguileta, M.A., Muise, S., Farazifard, R., Haque, M.E., McBride, H.M., Park, D.S., and Fon, E.A. (2012). Mitochondrial processing peptidase regulates PINK1 processing, import and Parkin recruitment. EMBO Rep. *13*, 378–385.

Haynes, C.M., Petrova, K., Benedetti, C., Yang, Y., and Ron, D. (2007). ClpP mediates activation of a mitochondrial unfolded protein response in C. elegans. Dev. Cell *13*, 467–480.

Haynes, C.M., Yang, Y., Blais, S.P., Neubert, T.A., and Ron, D. (2010). The matrix peptide exporter HAF-1 signals a mitochondrial UPR by activating the transcription factor ZC376.7 in C. elegans. Mol. Cell *37*, 529–540.

Jenkinson, E.M., Rehman, A.U., Walsh, T., Clayton-Smith, J., Lee, K., Morell, R.J., Drummond, M.C., Khan, S.N., Naeem, M.A., Rauf, B., et al.; University of Washington Center for Mendelian Genomics (2013). Perrault syndrome is caused by recessive mutations in CLPP, encoding a mitochondrial ATP-dependent chambered protease. Am. J. Hum. Genet. *92*, 605–613.

Kang, S.G., Dimitrova, M.N., Ortega, J., Ginsburg, A., and Maurizi, M.R. (2005). Human mitochondrial ClpP is a stable heptamer that assembles into a tetradecamer in the presence of ClpX. J. Biol. Chem. *280*, 35424–35432.

Keller, A., and Shteynberg, D. (2011). Software pipeline and data analysis for MS/MS proteomics: the trans-proteomic pipeline. Methods Mol. Biol. *694*, 169–189.

Ketela, T., Heisler, L.E., Brown, K.R., Ammar, R., Kasimer, D., Surendra, A., Ericson, E., Blakely, K., Karamboulas, D., Smith, A.M., et al. (2011). A comprehensive platform for highly multiplexed mammalian functional genetic screens. BMC Genomics *12*, 213.

Kimber, M.S., Yu, A.Y., Borg, M., Leung, E., Chan, H.S., and Houry, W.A. (2010). Structural and theoretical studies indicate that the cylindrical protease ClpP samples extended and compact conformations. Structure *18*, 798–808.

Kornblau, S.M., and Coombes, K.R. (2011). Use of reverse phase protein microarrays to study protein expression in leukemia: technical and methodological lessons learned. Methods Mol. Biol. *785*, 141–155.

Kornblau, S.M., Singh, N., Qiu, Y., Chen, W., Zhang, N., and Coombes, K.R. (2010). Highly phosphorylated FOXO3A is an adverse prognostic factor in acute myeloid leukemia. Clin. Cancer Res. *16*, 1865–1874.

Kornblau, S.M., Qiu, Y.H., Zhang, N., Singh, N., Faderl, S., Ferrajoli, A., York, H., Qutub, A.A., Coombes, K.R., and Watson, D.K. (2011). Abnormal expression of FLI1 protein is an adverse prognostic factor in acute myeloid leukemia. Blood *118*, 5604–5612.

Lagadinou, E.D., Sach, A., Callahan, K., Rossi, R.M., Neering, S.J., Minhajuddin, M., Ashton, J.M., Pei, S., Grose, V., O'Dwyer, K.M., et al. (2013). BCL-2 inhibition targets oxidative phosphorylation and selectively eradicates quiescent human leukemia stem cells. Cell Stem Cell *12*, 329–341.

Liu, G., Zhang, J., Larsen, B., Stark, C., Breitkreutz, A., Lin, Z.Y., Breitkreutz, B.J., Ding, Y., Colwill, K., Pasculescu, A., et al. (2010). ProHits: integrated software for mass spectrometry-based interaction proteomics. Nat. Biotechnol. *28*, 1015–1017.

Liu, G., Zhang, J., Choi, H., Lambert, J.P., Srikumar, T., Larsen, B., Nesvizhskii, A.I., Raught, B., Tyers, M., and Gingras, A.C. (2012). Using ProHits to store, annotate, and analyze affinity purification-mass spectrometry (AP-MS) data. In Current Protocols in Bioinformatics (John Wiley & Sons), pp. 8.16. 1–18.16. 32.

Montojo, J., Zuberi, K., Rodriguez, H., Kazi, F., Wright, G., Donaldson, S.L., Morris, Q., and Bader, G.D. (2010). GeneMANIA Cytoscape plugin: fast gene function predictions on the desktop. Bioinformatics *26*, 2927–2928.

Nicolini, F.E., Cashman, J.D., Hogge, D.E., Humphries, R.K., and Eaves, C.J. (2004). NOD/SCID mice engineered to express human IL-3, GM-CSF and Steel factor constitutively mobilize engrafted human progenitors and compromise human stem cell regeneration. Leukemia *18*, 341–347.

O'Connor, O.A., Stewart, A.K., Vallone, M., Molineaux, C.J., Kunkel, L.A., Gerecitano, J.F., and Orlowski, R.Z. (2009). A phase 1 dose escalation study of the safety and pharmacokinetics of the novel proteasome inhibitor carfilzomib (PR-171) in patients with hematologic malignancies. Clin. Cancer Res. *15*, 7085–7091.

Pierce, A., Whetton, A.D., Meyer, S., Ravandi-Kashani, F., Borthakur, G., Coombes, K.R., Zhang, N., and Kornblau, S. (2013). Transglutaminase

2 expression in acute myeloid leukemia: association with adhesion molecule expression and leukemic blast motility. Proteomics *13*, 2216–2224.

Richardson, P.G., Sonneveld, P., Schuster, M.W., Irwin, D., Stadtmauer, E.A., Facon, T., Harousseau, J.L., Ben-Yehuda, D., Lonial, S., Goldschmidt, H., et al.; Assessment of Proteasome Inhibition for Extending Remissions (APEX) Investigators (2005). Bortezomib or high-dose dexamethasone for relapsed multiple myeloma. N. Engl. J. Med. *352*, 2487–2498.

Roux, K.J., Kim, D.I., Raida, M., and Burke, B. (2012). A promiscuous biotin ligase fusion protein identifies proximal and interacting proteins in mammalian cells. J. Cell Biol. *196*, 801–810.

Shteynberg, D., Deutsch, E.W., Lam, H., Eng, J.K., Sun, Z., Tasman, N., Mendoza, L., Moritz, R.L., Aebersold, R., and Nesvizhskii, A.I. (2011). iProphet: multi-level integrative analysis of shotgun proteomic data improves peptide and protein identification rates and error estimates. Mol. Cell. Proteomics *10*, http://dx.doi.org/10.1074/mcp.M111.007690.

Simpson, C.D., Hurren, R., Kasimer, D., MacLean, N., Eberhard, Y., Ketela, T., Moffat, J., and Schimmer, A.D. (2012). A genome wide shRNA screen identifies α/β hydrolase domain containing 4 (ABHD4) as a novel regulator of anoikis resistance. Apoptosis *17*, 666–678.

Skrtić, M., Sriskanthadevan, S., Jhas, B., Gebbia, M., Wang, X., Wang, Z., Hurren, R., Jitkova, Y., Gronda, M., Maclean, N., et al. (2011). Inhibition of mitochondrial translation as a therapeutic strategy for human acute myeloid leukemia. Cancer Cell *20*, 674–688.

Tibes, R., Qiu, Y., Lu, Y., Hennessy, B., Andreeff, M., Mills, G.B., and Kornblau, S.M. (2006). Reverse phase protein array: validation of a novel proteomic technology and utility for analysis of primary leukemia specimens and hematopoietic stem cells. Mol. Cancer Ther. *5*, 2512–2521.

Vij, R., Wang, M., Kaufman, J.L., Lonial, S., Jakubowiak, A.J., Stewart, A.K., Kukreti, V., Jagannath, S., McDonagh, K.T., Alsina, M., et al. (2012). An open-label, single-arm, phase 2 (PX-171-004) study of single-agent carfilzomib in bortezomib-naive patients with relapsed and/or refractory multiple myeloma. Blood *119*, 5661–5670.

Xu, G.W., Ali, M., Wood, T.E., Wong, D., Maclean, N., Wang, X., Gronda, M., Skrtic, M., Li, X., Hurren, R., et al. (2010). The ubiquitin-activating enzyme E1 as a therapeutic target for the treatment of leukemia and multiple myeloma. Blood *115*, 2251–2259.

Zeiler, E., Korotkov, V.S., Lorenz-Baath, K., Böttcher, T., and Sieber, S.A. (2012). Development and characterization of improved β-lactone-based antivirulence drugs targeting ClpP. Bioorg. Med. Chem. *20*, 583–591.

Zhao, Q., Wang, J., Levichkin, I.V., Stasinopoulos, S., Ryan, M.T., and Hoogenraad, N.J. (2002). A mitochondrial specific stress response in mammalian cells. EMBO J. *21*, 4411–4419.